The Challenge of Characterizing Bimolecular Reactions of Aromatic Compounds via Computational Chemistry. the Case of the N(^{2}D) + Pyridine Reaction and Implications in the Chemistry of the Thermosphere of Titan

Luca Mancini[1(✉)], Marzio Rosi[2,3], and Nadia Balucani[1]

[1] Dipartimento di Chimica, Biologia e Biotecnologie, Università degli Studi di Perugia, 06123 Perugia, Italy
luca.mancini@unipg.it

[2] Dipartimento di Ingegneria Civile ed Ambientale, Università degli Studi di Perugia, 06125 Perugia, Italy

[3] Istituto CNR di Scienze e Tecnologie Chimiche "Giulio Natta" (CNR-SCITEC), 06123 Perugia, Italy

Abstract. Bimolecular reactions involving aromatic compounds are of great interest in many areas of applied science. Given their large weight, an experimental characterization might be difficult using the common experimental methods because of their low vapor pressure. Also the characterization via theoretical methods is difficult, because of the large number of atoms involved and some difficulty in describing delocalization effects with the usual methods for electronic structure calculations. In this contribution, we report a benchmark analysis of the reaction between pyridine and atomic nitrogen in the excited^{2}D state, which is of relevance in different fields in the chemistry of the thermosphere of Titan. We have used different computational strategies, mainly based on DFT methods, which represent a convenient option in the case of large systems. The use of more accurate methods, such as the coupled-cluster theory, might be difficult to implement considering the significant hardware requirements. The results of this analysis suggest that an acceptable computational strategy is represented by the use of hybrid functionals, such as the B3LYP or M062X, in conjunction with the aug-cc-pVTZ basis set. Implications for the chemistry of the atmosphere of Titan (the largest moon of Saturn) are briefly discussed.

Keywords: Theoretical Chemistry · DFT methods · Chemistry of Planetary Atmospheres

1 Introduction

The computational study of chemical reactions involving aromatic compounds represents a challenge to available theoretical methods. This is particularly true

© The Author(s), under exclusive license to Springer Nature Switzerland AG 2024
O. Gervasi et al. (Eds.): ICCSA 2024 Workshops, LNCS 14818, pp. 84–97, 2024.
https://doi.org/10.1007/978-3-031-65273-8_6

if the interest is directed at the reactions of polycyclic aromatic hydrocarbons (PAHs) and their functionalized derivatives given their aromatic nature and the large number of atoms involved. Nevertheless, the great interest in these species has motivated their study with the most advanced methods available (see, for example, the large amount of work carried out by Mebel and his collaborators [1–7]). Among other fields of application, a renewed interest in the chemistry of PAHs and their functionalized derivatives has emerged in the context of astrochemistry and cosmochemistry. Indeed, PAHs and their derivatives have been identified in many extraterrestrial environments, from the interstellar medium [8–10] to comets [11–13] (including 67P/Churyumov-Gerasimenko [14]), carbonaceous chondrites [15], micrometeorites [16] and even in the pristine sample of the carbonaceous asteroid (162173) Ryugu collected by the Hayabusa2 mission [17].

For this reason, in our laboratory we have recently started a systematic investigation of some reactions involving aromatic compounds and atomic nitrogen in its first electronically excited ^{2}D state [18–22]. These reactions are relevant to the chemistry of the thermosphere of Titan, the massive moon of Saturn, that has long attracted great interest in the study of prebiotic chemistry on a planetary scale [23–26]. We started from the reaction of N(^{2}D) with benzene (the simplest aromatic compound) as it was suggested as a possible route for the formation of pyridine [18,19], an organic molecule simple enough to form in an abiotic environment but with a notable prebiotic potential given the number of biomolecules characterized by its structure (e.g. niacin, pyridoxine, and nicotinamide adenine dinucleotide). The suggested mechanism, involving a N/CH exchange reaction, was found to be open according to our calculations of the potential energy surface (PES) [19]. However, the competition with other reaction channels makes that channel minor as demonstrated by an experimental study and further theoretical work by us [22] and Chin et al. [27] in which estimates of the product branching fractions (BFs) were obtained via Rice-Ramsperger-Kassel-Marcus (RRKM) theory. Quite surprisingly, the main reaction channel of the N(^{2}D) + benzene reaction is a ring contraction channel associated with the formation of cyclopentadienyl and HCN while minor contributions come from the channels leading to o-N-cycloheptatriene radical + H, pyrrolyl + acetylene and cyanocyclopentadiene + H [22,27].

The presence of pyridine and pyrimidine in the upper atmosphere of Titan was suggested by the analysis of the Cassini Ion Neutral Mass Spectrometer data, but ground-based attempts to detect it by using ALMA could not confirm their presence and only upper limits of their abundances were derived [24]. To be noted that polycyclic aromatic hydrocarbons (PAHs) and N-containing PAHs have been invoked [28] to explain an unidentified emission band near 3.28 μm analyzed by Dinelli et al. [29]. Furthermore, the Cassini plasma spectrometer ion beam spectrometer data analysis strongly suggests that PAHs and N-containing PAHs account for the ion signal recorded at 170–310 Da [30]. Even if not a single PAH/N-PAH was identified, it seems quite clear that if N-PAHs are present in

the thermosphere of Titan, some formation mechanism must be active. N(^{2}D) reactions with PAHs may be a viable route.

For the above reasons, we have also explored the title reaction that features N(^{2}D) and pyridine as reactants (incidentally, if the N/CH exchange channel is competitive, pyrimidine could be the formed product). In this case as well, experimental data obtained in crossed molecular beam experiments are available [31] and a comparison between experimental and theoretical BFs is being pursued (Mancini et al., in preparation). Both the cases of N(^{2}D) + benzene [22] and, in this work, N(^{2}D) + pyridine have been investigated at a high level of theory. We performed CCSD(T) calculations, extrapolating to complete basis set and including core-valence correlation effects. However, these calculations were extremely costly in terms of CPU time and disk space requirements. Going towards less symmetric and larger systems, it is not possible to perform similar calculations both for the computer time required and the scratch disk space necessary. Therefore, it is necessary to find a compromise between the accuracy of the calculations and their computational costs.

In this contribution, we present a benchmark study of the title reaction only for a portion of the global PES that will be the object of a future paper. In particular, we have considered only one of the possible initial steps of the reaction. Different theoretical methods have been employed to characterize the energetics of the reactants, products, intermediates and transition states along that portion of the PES. The system is much more complex than the reaction with benzene, even though benzene and pyridine are isoelectronic, because of the symmetry loss once N is present in the aromatic ring. The benchmark will be a way to establish which DFT method works better for these type of reactive systems and it will be used to study the reactions of N(^{2}D) with large PAHs.

2 Theoretical Methods: Electronic Structure Calculations

To assess the best computational strategy, a benchmark study has been performed. In detail, following the same approach already used for the characterization of reactions of N(^{2}D) with different hydrocarbons [22,32–34], geometry optimization has been performed at the DFT level. Different functionals have been employed, including the B3LYP-D3, ωB97XD, and the M062X, using both the 6–311++G(d,p) Pople's basis set and the correlation consistent valence polarized set aug-cc-pVTZ. Harmonic vibrational frequencies have been calculated using the same level of theory of geometry optimization. The zero point correction obtained has been then used to correct the energies of each stationary point. Finally, IRC calculations [35,36] allowed the identification of the saddle points. The obtained data have been compared with a standard reference, consisting of accurate single-point energy calculations, performed at the coupled-cluster (CCSD(T)) level, corrected with a Density Fitted (DF)MP2 extrapolation to the complete basis set (CBS) and with corrections for core electrons excitations. The scheme of the energy extrapolation is:

$$E = E(CCSD(T)/aug-cc-pVTZ)+ \\ [E(CCSD(T,core)/cc-pVTZ) - E(CCSD(T)/cc-pVTZ)] \\ + [E(DF-MP2/CBS) - E(DF-MP2/aug-cc-pVTZ)]$$

where E(DF-MP2/CBS) is defined as:

$$E(DF-MP2/CBS) = E[(DF-MP2)/aug-cc-pVQZ)]+ \\ 0.5772 * [E(DF-MP2/aug-cc-pVQZ) \\ - E(DF-MP2/aug-cc-pVTZ)]$$

where the E(DF-MP2/CBS) extrapolation has been performed using Martin's two parameter scheme [37]. The results obtained have been corrected considering the zero point energy evaluated at the B3LYP-D3/aug-cc-pVTZ level of theory. All the energy values have been rounded to 1 kJ/mol, to be consistent with the"chemical accuracy" of 1 kcal/mol. The first electronic excited state of atomic nitrogen, N(^{2}D), is difficult to treat through single-reference methods, due to an overlapping between different spin states during the calculations. For this reason, the energy of N(^{2}D) has been estimated by adding the experimental N(^{4}S)-N(^{2}D) separation of 230 kJ/mol [38] to the energy of N(^{4}S) calculated in the present work. The Gaussian09 and Molpro suits of programs have been used to perform electronic structure calculations [39,40].

3 Results

3.1 Potential Energy Surface

The portion of the potential energy surface (PES) resulting from the theoretical investigation is reported in Fig. 1. The energy values reported in the scheme are those evaluated at the CCSD(T)/CBS level of theory.

The initial step of the reaction is represented by the interaction of N(^{2}D) with the π-system of the pyridine molecule. The addition can occur in different positions (ortho, meta, para, and ipso). Here we consider the portion of the PES that is accessed after the addition in the meta/para position with the formation of an intermediate (MIN1) characterized by the presence of a three-member-ring moiety. The process is barrierless and the relative energy of the intermediate is -329 kJ/mol. The breaking of a C-C bond and the "sliding" of the N atom into the ring leads to the formation of a seven-member ring intermediate (MIN2, located 432 kJ/mol below the reactant energy asymptote). A small barrier of 10 kJ/mol must be overcome during the process. Alternatively, a different isomerization process is responsible for the formation of the MIN3 intermediate (located at -527 kJ/mol with respect to the reactants asymptote) via the H-migration and formation of a N-H bond. In this case, the barrier,

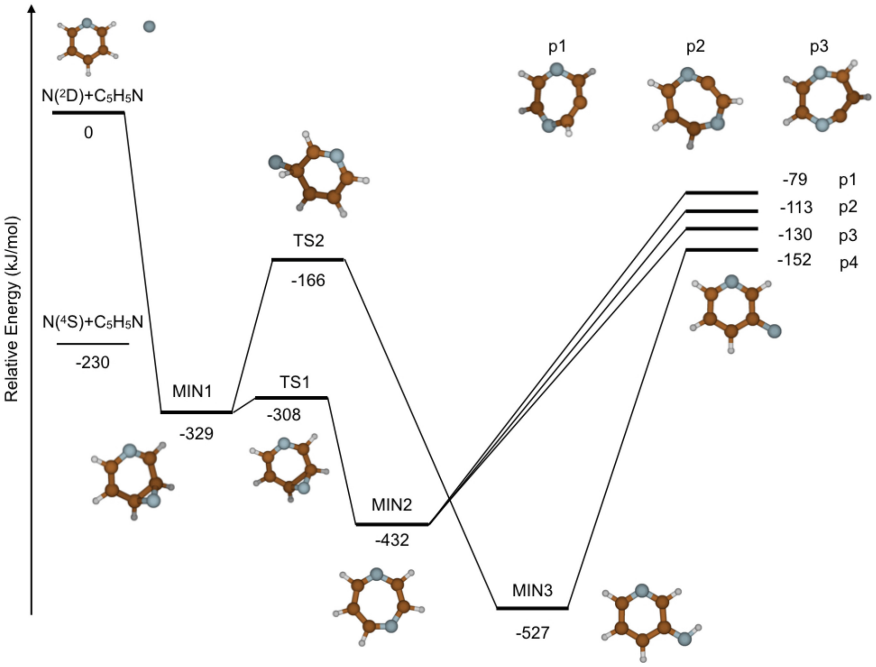

Fig. 1. 2D scheme of the PES obtained for the N(^{2}D)+pyridine reaction.

represented by the TS2 saddle point, is higher (163 kJ/mol) than that associated to the other isomerization process. Therefore, this pathway is expected to be less competitive. Once formed, the MIN2 intermediate can directly decompose, through a H-displacement process. Due to the loss of symmetry with respect to the case of benzene, the H atom can be released from three different positions and three different isomeric products can be formed. The enthalpy change associated with the three product channels (p1, p2 and p3) is -79 kJ/mol, -113 kJ/mol and -130 kJ/mol, respectively. Also the MIN3 intermediate can lose one H atom, leading to the formation of the p4 co-fragment, a radical in a triplet spin state. All H-loss processes are barrierless, that is, the dissociation takes place without the presence of a saddle point in the exit channel.

3.2 Benchmark Analysis

As described above (see Sect. 2), DFT calculations have been performed using different functionals and basis sets to establish the best computational strategy for the analysis of the PES. Both the energies and the geometrical parameters have been compared. In detail, the geometrical analysis has been focused on three stationary points representative of different scenarios, the pyridine molecule (representing a singlet closed-shell molecule) and two open-shell structures: MIN2, being a seven-member ring in the doublet electronic state, and the TS1 sad-

dle point. In Fig. 2 are reported the structures of the stationary points with the labeled bonds object of the study, while in Table 1, the values of the bond lengths (in Å) obtained at different levels of theory are listed.

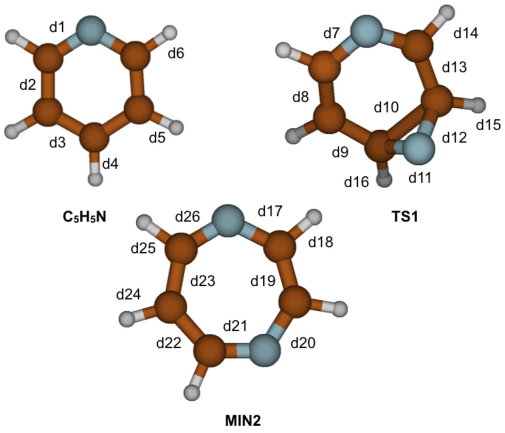

Fig. 2. Structure of the three stationary points used to compare the geometrical parameters, resulting from the theoretical analysis.

As can be seen from the data presented in Table 1, the differences in the values of bond lengths are very small (almost negligible), even considering the use of a more accurate basis set (i.e., the aug-cc-pVTZ). Therefore, the only comparison of the bond distances is not sufficient to select the most appropriate computational strategy. For this reason, the energies of all the stationary points identified have been evaluated. In the first instance, the zero point energy correction, derived from the frequency calculations can be analysed. As can be seen from Table 2, small differences between the various levels of theory are present. The main deviation in the case of the pyridine molecule is 0.0010 Hartree/particles, which corresponds to 2.74 kJ/mol and is lower than the chemical accuracy. One of the main deviations can be appreciated in the case of the MIN1 intermediate, where the major difference is obtained comparing the B3LYP/6–311++G(d,p) and the ωB97XD/aug-cc-pVTZ level, leading to a value of 0.0017 Hartree/particles (equal to 4.59kJ/mol, barely around the limit value of chemical accuracy of 1 kcal/mol).

The relative energy with respect to the reactant asymptote (taken as zero reference) obtained at the various levels of theory is reported in Table 3. Those values reported include the zero-point corrections (evaluated at the same level of theory used for the geometry optimization). The comparison is done with the more accurate CCSD(T)/CBS data. It can be noticed how the use of a bigger basis set, i.e., the aug-cc-pVTZ, leads to values more in line with the complete basis set extrapolation limit. All three functionals provide similar results, with small deviations. The main differences can be appreciated in the case of p4

Table 1. Bond lengths (in *Å*) evaluated for the main distances in the structures reported in Fig. 2, where *6–311* and *TZ* represent the 6–311++G(d,p) and aug-cc-pVTZ basis sets, respectively.

Dist	B3LYP-D3/	B3LYP-D3/	ωB97XD/	ωB97XD/	M062X/	M062X/
	6–311	TZ	6–311	TZ	6–311	TZ
d1	1.337	1.334	1.332	1.330	1.332	1.330
d2	1.395	1.391	1.390	1.386	1.392	1.388
d3	1.393	1.388	1.388	1.385	1.389	1.386
d4	1.084	1.082	1.084	1.082	1.084	1.082
d5	1.084	1.081	1.084	1.081	1.083	1.081
d6	1.086	1.084	1.086	1.084	1.086	1.084
d7	1.354	1.351	1.343	1.341	1.342	1.339
d8	1.377	1.373	1.378	1.375	1.372	1.379
d9	1.421	1.417	1.408	1.404	1.404	1.400
d10	1.792	1.785	1.824	1.820	1.835	1.832
d11	1.415	1.412	1.404	1.402	1.407	1.406
d12	1.419	1.416	1.411	1.409	1.413	1.412
d13	1.423	1.420	1.409	1.405	1.406	1.402
d14	1.088	1.086	1.088	1.085	1.087	1.085
d15	1.090	1.087	1.089	1.086	1.088	1.086
d16	1.089	1.087	1.089	1.086	1.088	1.086
d17	1.379	1.376	1.376	1.373	1.376	1.373
d18	1.087	1.085	1.087	1.084	1.086	1.085
d19	1.371	1.367	1.365	1.361	1.367	1.363
d20	1.379	1.376	1.376	1.373	1.376	1.373
d21	1.314	1.312	1.310	1.307	1.309	1.307
d22	1.413	1.409	1.409	1.405	1.411	1.407
d23	1.413	1.409	1.409	1.405	1.411	1.407
d24	1.085	1.082	1.085	1.082	1.083	1.081
d25	1.091	1.088	1.091	1.088	1.090	1.088
d26	1.314	1.312	1.310	1.307	1.309	1.307

and MIN3. The reason for such a difference is due to correlation effects in the case of the presence of a multi-reference character of the stationary points, as can be seen from the value of the T1 diagnostic parameter of 0.028 and 0.027, respectively. As reported in previous studies [41,42], a value of T1 higher than 0.02 leads to a strong multi-reference character, which can be properly taken into account by using different methods (including CASSCF and/or CASPT2).

Table 2. Zero-point energy correction (in Hartree/particle) calculated for the main stationary points in the PES at different levels of theory. *6–311* and *TZ* represent the 6–311++G(d,p) and aug-cc-pVTZ basis sets, respectively.

Point	**B3LYP-D3/ 6–311**	**B3LYP-D3/ TZ**	**ωB97XD/ 6–311**	**ωB97XD/ TZ**	**M062X/ 6–311**	**M062X/ TZ**
C_5H_5N	0.088376	0.088596	0.089275	0.089421	0.089223	0.089338
MIN1	0.090302	0.090424	0.091870	0.092049	0.091831	0.091940
MIN2	0.090208	0.0900470	0.091194	0.091412	0.090666	0.090967
MIN3	0.091410	0.091642	0.092312	0.092569	0.092189	0.092424
TS1	0.088964	0.089087	0.090248	0.090333	0.090185	0.0900221
TS2	0.084813	0.084910	0.086491	0.087686	0.085602	0.085733
p1	0.079424	0.079542	0.080665	0.080719	0.080751	0.080833
p2	0.079390	0.079507	0.080570	0.080646	0.080734	0.080760
p3	0.079188	0.079291	0.080403	0.080467	0.0880411	0.080452
p4	0.078815	0.079076	0.079593	0.079853	0.079735	0.079981

Table 3. Relative energies (in kJ/mol) obtained for the main stationary points in the PES at different levels of theory. B3 = B3LYP-D3 6–311 = 6–311++G(d,p) TZ = aug-cc-pVTZ ωB = ωB97XD M06 = M062X

Point	**B3/ 6–311**	**B3/ TZ**	**ωB/ 6–311**	**ωB/ TZ**	**M06/ 6–311**	**M06/ TZ**	**CCSD(T)/ CBS**
MIN1	-335	-332	-331	-335	-330	-337	-329
MIN2	-460	-454	-436	-442	-424	-432	-432
MIN3	-549	-542	-531	-536	-517	-524	-527
TS1	-328	-322	-313	-319	-309	-316	-308
TS2	-169	-163	-117	-122	-138	-154	-166
p1	-117	-109	-94	-101	-100	-109	-113
p2	-137	-129	-114	-122	-122	-132	-130
p3	-79	-73	-56	-62	-60	-67	-79
p4	-184	-180	-170	-172	-156	-161	-152

In general, to characterize the reaction mechanism and predict the product branching fractions, it is important to derive the minimum energy path for all competing reaction channels. The presence of a series of energy barriers can promote or hinder certain reaction paths, leading to an appreciable effect on the final reaction micro-mechanism. In Table 4 are reported the enthalpy changes and the barrier heights (in kJ/mol) for the different reaction paths, leading to the various product channels identified in the PES.

As can be noticed, the B3LYP functional (together with the M062X one), in conjunction with the aug-cc-pVTZ basis set, provides results in line with the

Table 4. Enthalpy changes (ΔH_0^0) and Barrier Heights, reported in kJ/mol, for the reaction pathways in the PES, evaluated at different levels of theory. B3 = B3LYP-D3 TZ = aug-cc-pVTZ ωB = ωB97XD M06 = M062X CBS = CCSD(T)/CBS

Path	B3/TZ		ω B/TZ		M06/TZ		CBS	
	ΔH_0^0	Barrier	ΔH_0^0	Barrier	ΔH_0^0	Barrier	ΔH_0^0	Barrier
C_5H_5N →MIN1	-332	-	-337	-	-337	-	-329	-
MIN1 → MIN2	-122	10	-105	18	-95	21	-103	21
MIN1 → MIN3	-211	169	-199	215	-187	192	-198	163
MIN2 →p1	381	-	380	-	365	-	353	-
MIN2 →p2	345	-	341	-	323	-	319	-
MIN2 →p3	325	-	320	-	300	-	302	-
MIN3 → p4	363	-	364	-	363	-	375	-

accurate CCSD(T)/CBS reference. It represents also a useful strategy for the optimization of the stationary points in terms of CPU time. In general the differences in the values of energy are not expected to contribute significantly, also in the case of MIN3 and TS2 (which shows a strong multi-reference character), since the relative heights and the paths probability are basically unchanged. This is at variance with the case of the reactions involving atomic oxygen, where the presence of open-shell species with unpaired electrons (both in the singlet and in the triplet state) can alter the energy (and, consequently, the morphology) of the PES [43–45]. In some cases, indeed the strong multi-reference character of some stationary points identified in the PES required the refinement of the energy of minima and transition states at a higher level of theory (such as the CASPT2).

4 Conclusions

The present contribution reports a benchmark study on the reaction between atomic nitrogen, in its first electronically excited ^{2}D state, and the pyridine molecule when considering the addition of N in the meta/para positions. A more complete work is currently underway (Mancini et al., in preparation). The theoretical branching fractions of the products will be obtained considering all the possible addition sites and a comparison with the experimental results by [31] will be carried out. In this work, different DFT methods have been considered and compared with the predictions of the more accurate CCSD(T) theory with the extrapolation on the complete basis set limit. In general, one of the best choices for the estimate of the energies is the use of correlation methods (such as CCSD(T)) but in the cases in which the dimensions of the system are too large, it is difficult to use because of the high computational cost. All the methods used here provide similar results in the case of geometry optimization. The more accurate aug-cc-pVTZ basis set can be considered a better alternative to the 6–311++G(d,p) Pople's basis set since it provides, as expected, more

accurate results. A more general conclusion is that the energy values determined at the DFT level can be used to represent the competing reaction channels in the potential energy surface, providing that the energy values associated with the transition states and reaction intermediates homogeneously scale. In this way, albeit differing with respect to the reference value, the relative probability of the occurrence of each channel remains unchanged. The data obtained at the DFT level can be considered a good starting point for a kinetic analysis, which allows us to derive the product branching fractions. Among the plethora of available DFT functionals, the B3LYP appears to be a good compromise between chemical accuracy and computational cost for the analysis of the PES.

After this benchmark work, we will apply the B3LYP method to the theoretical characterization of reactions involving N(^{2}D) (and also other atomic and radical species) with larger aromatic species, like naphthalene and indene (which are supposed to be intermediate steps toward the formation of more complex PAHs starting from benzene), as well as N-PAHs, like quinoline and 1,3,5 triazine, or other aromatic species that have been speculated to be present in the upper atmosphere of Titan [28,30]. For some of those systems, the comparison with the experimental results obtained by the crossed molecular beam method will allow us to verify if the level of calculations is appropriate. If necessary, we will resort to the higher-level calculations. This combined experimental and theoretical work is necessary because the crossed molecular beam method nicely reproduces the low-pressure environment of the upper atmosphere of Titan, but not its low temperature. Therefore, the theoretical predictions, once validated by the comparison with the experimental results at high collision energies, will be extended to the temperatures relevant to the very cold moon of Saturn as was done in previous work by us [46–50]. Those results will contribute to a thorough understanding of the rich atmospheric chemistry of Titan [24].

Acknowledgements. This work was supported by the Italian Space Agency (Bando ASI Prot. n. DC-DSR-UVS-2022-231, Grant no. 2023-10-U.0 "Modeling Chemical Complexity: all'Origine di questa e di altre Vite per una visione aggiornata delle missioni spaziali (MIGLIORA)" Codice Unico di Progetto (CUP) F83C23000800005). M. Rosi also acknowledge financial support under the National Recovery and Resilience Plan (NRRP), Mission 4, Component 2, Investment 1.1, Call for tender No. 104 published on 2.2.2022 by the Italian Ministry of University and Research (MUR), funded by the European Union - NextGenerationEU- Project Title 2022JC2Y93 ChemicalOrigins: linking the fossil composition of the Solar System with the chemistry of protoplanetary disks - CUP J53D23001600006 - Grant Assignment Decree No. 962 adopted on 30.06.2023 by the Italian Ministry of Ministry of University and Research (MUR).

References

1. Kaiser, R.I., Parker, D.S., Mebel, A.M.: Reaction dynamics in astrochemistry: low-temperature pathways to polycyclic aromatic hydrocarbons in the interstellar medium. Annu. Rev. Phys. Chem. **66**, 43–67 (2015)
2. Parker, D.S., et al.: Low temperature formation of naphthalene and its role in the synthesis of PAHs (polycyclic aromatic hydrocarbons) in the interstellar medium. Proc. Natl. Acad. Sci. **109**(1), 53–58 (2012)
3. Yang, T., et al.: Hydrogen-abstraction/acetylene-addition exposed. Angew. Chem. Int. Ed. **55**(48), 14983–14987 (2016)
4. Zhao, L., et al.: Pyrene synthesis in circumstellar envelopes and its role in the formation of 2D nanostructures. Nature Astron. **2**(5), 413–419 (2018)
5. Kaiser, R., Parker, D., Zhang, F., Landera, A., Kislov, V., Mebel, A.: PAH formation under single collision conditions: reaction of phenyl radical and 1, 3-butadiene to form 1, 4-dihydronaphthalene. J. Phys. Chem. A **116**(17), 4248–4258 (2012)
6. Kislov, V., Sadovnikov, A., Mebel, A.: Formation mechanism of polycyclic aromatic hydrocarbons beyond the second aromatic ring. J. Phys. Chem. A **117**(23), 4794–4816 (2013)
7. Frenklach, M., Mebel, A.M.: On the mechanism of soot nucleation. Phys. Chem. Chem. Phys. **22**(9), 5314–5331 (2020)
8. Allamandola, L., Tielens, A., Barker, J.: Polycyclic aromatic hydrocarbons and the unidentified infrared emission bands-auto exhaust along the Milky Way. Astrophys. J. Part 2-Lett. Editor (ISSN 0004-637X), vol. 290, March 1, 1985, p. L25–L28. **290**, L25–L28 (1985)
9. Allamandola, L., Tielens, A., Barker, J.: Interstellar polycyclic aromatic hydrocarbons-The infrared emission bands, the excitation/emission mechanism, and the astrophysical implications. Astrophys. J. Suppl. Ser. (ISSN 0067–0049), vol. 71, Dec. 1989, p. 733–775. Res. support. NASA DOE NSF. **71**, 733–775 (1989)
10. Tielens, A.G.: Interstellar polycyclic aromatic hydrocarbon molecules. Annu. Rev. Astron. Astrophys. **46**, 289–337 (2008)
11. Moreels, G., Clairemidi, J., Hermine, P., Brechignac, P., Rousselot, P.: Detection of a polycyclic aromatic molecule in comet P/Halley. Astron. Astrophys. (ISSN 0004-6361), vol. 282, no. 2, p. 643–656 **282**, 643–656 (1994)
12. McKay, A.J., Roth, N.X.: Organic matter in cometary environments. Life **11**(1), 37 (2021)
13. Clemett, S.J., Sandford, S.A., Nakamura-Messenger, K., Horz, F., McKAY, D.S.: Complex aromatic hydrocarbons in stardust samples collected from comet 81P/wild 2. Meteorit. Planet. Sci. **45**(5), 701–722 (2010). https://doi.org/10.1111/j.1945-5100.2010.01062.x, https://onlinelibrary.wiley.com/doi/abs/10.1111/j.1945-5100.2010.01062.x
14. Hänni, N., et al.: Identification and characterization of a new ensemble of cometary organic molecules. Nat. Commun. **13**(1), 3639 (2022)
15. Spencer, M.K., Hammond, M.R., Zare, R.N.: Laser mass spectrometric detection of extraterrestrial aromatic molecules: mini-review and examination of pulsed heating effects. Proc. Natl. Acad. Sci. **105**(47), 18096–18101 (2008)
16. Maurette, M.: Carbonaceous micrometeorites and the origin of life. Orig. Life Evol. Biosph. **28**(4), 385–412 (1998)
17. Naraoka, H., et al.: Soluble organic molecules in samples of the carbonaceous asteroid (162173) Ryugu. Science **379**(6634), eabn9033 (2023)

18. Balucani, N., Pacifici, L., Skouteris, D., Caracciolo, A., Casavecchia, P., Rosi, M.: A theoretical investigation of the reaction N(2D) + C6H6 and implications for the upper atmosphere of titan. In: Gervasi, O., et al. Computational Science and Its Applications – ICCSA 2018. ICCSA 2018. LNCS, vol. 10961. Springer, Cham (2018). https://doi.org/10.1007/978-3-319-95165-2_53
19. Balucani, N., Pacifici, L., Skouteris, D., Caracciolo, A., Casavecchia, P., Falcinelli, S., Rosi, M.: A computational study of the reaction n (2 d)+ c 6 h 6 leading to pyridine and phenylnitrene. In: Computational Science and Its Applications–ICCSA 2019: 19th International Conference, Saint Petersburg, Russia, July 1–4, 2019, Proceedings, Part III 19. pp. 316–324. Springer (2019)
20. Rosi, M., et al.: A computational study on the insertion of N (2 D) into a C-H or C-C bond: the reactions of N (2 D) with benzene and toluene and their implications on the chemistry of titan. In: Computational Science and Its Applications–ICCSA 2020: 20th International Conference, Cagliari, Italy, July 1–4, 2020, Proceedings, Part III 20, pp. 744–755. Springer (2020). https://doi.org/10.1007/978-3-030-58808-3_54
21. Rosi, M., et al.: A Computational study of the reaction between N(2D) and simple aromatic hydrocarbons. In: Gervasi, O., et al. (eds.) Computational Science and Its Applications – ICCSA 2023 Workshops: Athens, Greece, July 3–6, 2023, Proceedings, Part II, pp. 718–734. Springer Nature Switzerland, Cham (2023). https://doi.org/10.1007/978-3-031-37108-0_46
22. Balucani, N., et al: An experimental and theoretical investigation of the N(2D) + C6H6 (benzene) reaction with implications for the photochemical models of Titan . Faraday Discuss. **245**, 327–351 (2023). https://doi.org/10.1039/D3FD00057E
23. Sagan, C., Thompson, W.R., Khare, B.N.: Titan: a laboratory for prebiological organic chemistry. Acc. Chem. Res. **25**(7), 286–292 (1992). https://doi.org/10.1021/ar00019a003
24. Nixon, C.A.: The Composition and chemistry of Titan's atmosphere. ACS Earth Space Chem. **8**(3), 406–456 (2024). https://doi.org/10.1021/acsearthspacechem.2c00041
25. Vuitton, V., Dutuit, O., Smith, M.A., Balucani, N.: Chemistry of titan's atmosphere. In: Müller-Wodarg, I., Griffith, C.A., Lellouch, E., Cravens, T.E. (eds.) Titan: Interior, Surface, Atmosphere, and Space Environment, pp. 224–284. Cambridge University Press (2014). https://doi.org/10.1017/CBO9780511667398.010
26. Balucani, N.: Elementary reactions of N atoms with hydrocarbons: first steps towards the formation of prebiotic N-containing molecules in planetary atmospheres. Chem. Soc. Rev. **41**(16), 5473 (2012). https://doi.org/10.1039/c2cs35113g
27. Chin, C.-H., Zhu, T., Zhang, J.Z.H.: Cyclopentadienyl radical formation from the reaction of excited nitrogen atoms with benzene: a theoretical study. Phys. Chem. Chem. Phys. **23**(21), 12408–12420 (2021). https://doi.org/10.1039/D1CP00133G
28. López-Puertas, M., et al.: Large abundances of polycyclic aromatic hydrocarbons in titan's upper atmosphere. Astrophys. J. **770**(2), 132 (2013)
29. Dinelli, B., et al.: An unidentified emission in titan's upper atmosphere. Geophys. Res. Lett. **40**(8), 1489–1493 (2013)
30. Haythornthwaite, R.P., et al.: Heavy positive ion groups in titan's ionosphere from cassini plasma spectrometer IBS observations. Planet. Sci. J. **2**(1), 26 (2021)
31. Recio, P., et al.: A crossed molecular beam investigation of the N (2D)+ pyridine reaction and implications for prebiotic chemistry. Chem. Phys. Lett. **779**, 138852 (2021)

32. Vanuzzo, G., et al.: Reaction N (2D)+ CH2CCH2 (Allene): an experimental and theoretical investigation and implications for the photochemical models of titan. ACS Earth Space Chem. **6**(10), 2305–2321 (2022)
33. Mancini, L., et al.: The reaction N (2D)+ CH3CCH (methylacetylene): a combined crossed molecular beams and theoretical investigation and implications for the atmosphere of titan. J. Phys. Chem. A **125**(40), 8846–8859 (2021)
34. Vanuzzo, G., et al.: The N(2D)+ CH2CHCN (vinyl cyanide) reaction: a combined crossed molecular beam and theoretical study and implications for the atmosphere of titan. J. Phys. Chem. A **126**(36), 6110–6123 (2022)
35. Gonzalez, C., Schlegel, H.B.: An improved algorithm for reaction path following. J. Chem. Phys. **90**(4), 2154–2161 (1989). https://doi.org/10.1063/1.456010
36. Gonzalez, C., Schlegel, H.B.: Reaction path following in mass-weighted internal coordinates. J. Phys. Chem. **94**(14), 5523–5527 (1990). https://doi.org/10.1021/j100377a021
37. Martin, J.M.: Ab initio total atomization energies of small molecules-towards the basis set limit. Chem. Phys. Lett. **259**(5–6), 669–678 (1996)
38. Moore, C.E.: Atomic Energy Levels. National Bureau of Standards, US Department of Commerce (1949)
39. Frisch, M., et al.: Gaussian 09, Revision A. 02, 2009, Gaussian. Inc., Wallingford CT (2009)
40. Werner, H.J., et al.: The molpro quantum chemistry package. J. Chem. Phys. **152**(14), 144107 (2020)
41. Leonori, F., et al.: Experimental and theoretical studies on the dynamics of the O(3P)+ propene reaction: primary products, branching ratios, and role of intersystem crossing. J. Phys. Chem. C **119**(26), 14632–14652 (2015)
42. Gimondi, I., Cavallotti, C., Vanuzzo, G., Balucani, N., Casavecchia, P.: Reaction dynamics of O(3P)+ propyne: Ii. primary products, branching ratios, and role of intersystem crossing from ab initio coupled triplet/singlet potential energy surfaces and statistical calculations. J. Phys. Chem. A **120**(27), 4619–4633 (2016)
43. Recio, P., et al.: Intersystem crossing in the entrance channel of the reaction of O(3P) with pyridine. Nat. Chem. **14**(12), 1405–1412 (2022)
44. Balucani, N., et al.: Crossed molecular beam experiments and theoretical simulations on the multichannel reaction of toluene with atomic oxygen. Faraday Discuss. (2024)
45. Pannacci, G., et al.: A combined crossed molecular beam and theorerical study of the O (3 P, 1 D)+ acrylonitrile (CH 2 CHCN) reactions and implications for combustion and extraterrestrial environments. Phys. Chem. Chem. Phys. **25**(30), 20194–20211 (2023)
46. Balucani, N., et al.: Combined crossed molecular beam and theoretical studies of the N (2D)+ CH4 reaction and implications for atmospheric models of titan. J. Phys. Chem. A **113**(42), 11138–11152 (2009)
47. Balucani, N., et al.: Formation of nitriles and imines in the atmosphere of titan: combined crossed-beam and theoretical studies on the reaction dynamics of excited nitrogen atoms N(2D) with ethane. Faraday Discuss. **147**, 189–216 (2010)
48. Balucani, N., et al.: Combined crossed beam and theoretical studies of the N(2D)+ C2H4 reaction and implications for atmospheric models of titan. J. Phys. Chem. A **116**(43), 10467–10479 (2012)

49. Liang, P., et al.: Combined crossed molecular beams and computational study on the N(2D)+ HCCCN (x1σ+) reaction and implications for extra-terrestrial environments. Mol. Phys. **120**(1–2), e1948126 (2022)
50. Mancini, L., et al.: A computational characterization of the reaction mechanisms for the reactions N(2D)+ CH3CN and hc3n and implications for the nitrogen-rich organic chemistry of titan. Comput. Theor. Chem. **1229**, 114341 (2023)